Conference on Modelling Fluid Flow (CMFF'22)
The 18th International Conference on Fluid Flow Technologies
Budapest, Hungary, August 30-September 2, 2022

Numerical simulation of a confined backward-facing step flow using hybrid turbulence models in OpenFOAM

Wim MUNTERS[†,1], Lilla KOLOSZAR[1], Philippe PLANQUART[1]

[1] Department of Environmental and Applied Fluid Dynamics. von Karman Institute for Fluid Dynamics. Waterloosesteenweg 72, 1640 Sint-Genesius-Rode, Belgium.
[†]Corresponding author. Email: wim.munters@vki.ac.be

ABSTRACT

To date, numerical simulation of separated flows remains challenging, with hybrid RANS–LES turbulence models promising to deliver scale-resolving accuracy at acceptable computational cost. Here, we investigate hybrid turbulence models readily available in OpenFOAM, and benchmark their performance to Reynolds-averaged approaches and turbulence-resolving high-fidelity reference data for a confined backward-facing step flow at low Reynolds number. Results show that scale-adaptive simulation techniques do not produce resolved turbulence and fail to outperform the baseline Reynolds-averaged simulations for the considered case. In contrast, detached-eddy variants do resolve turbulence in the separated shear layer, yet some configurations suffer from modelled-stress depletion. A grid coarsening study compares the degradation of accuracy for each approach, showcasing robustness of the standard Reynolds-averaged approach and, surprisingly, the relatively good performance of full large-eddy simulations even at coarse resolutions.

Keywords: Backward-facing step, Detached Eddy Simulation, Hybrid turbulence modelling, Large-eddy simulation, OpenFOAM, Scale-adaptive simulation

1. INTRODUCTION

Hybrid turbulence models, in which different modeling strategies are applied throughout the simulation domain, have historically been used primarily for high-Reynolds number external flows around airfoils and obstacles with massive separation in fields such as aerospace and ground transportation [1, 2]. Since the late 1990s, a large amount of different hybrid models based on Reynolds-Averaged Navier–Stokes (RANS) and Large-Eddy Simulation (LES) models have been developed based on various techniques for hybridization. Recent overviews of the general approach and state-of-the-art methods can be found, e.g., in [3]. Although they have been used with success in many studies, several weaknesses have also become apparent over the years. For example, spurious switching to LES zones in insufficiently destabilized regions has been known to produce so-called modeled stress depletion (MSD), in which neither modeled (RANS) nor resolved (LES) turbulence produces sufficient mixing close to transition zones [1]. Furthermore, studies using hybrid turbulence models for internal flows at low to medium Reynolds numbers have been more scarce to date. Even though such cases benefit from (partial) scale resolution, effects of viscosity and confinement have the potential to attenuate massive separation effects as observed in high-Reynolds external flows, which can be challenging for hybrid methods [1].

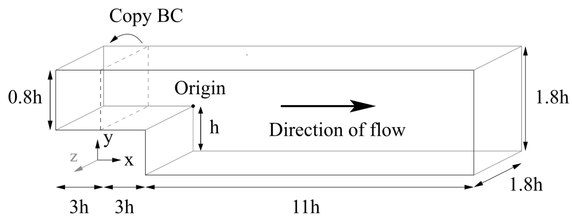

Figure 1. Sketch of the BFS domain. Figure adapted from [4]

Here, we investigate hybrid turbulence models available in OpenFOAM, and benchmark their performance to fully Reynolds-averaged approaches, LES with partial scale resolution, and direct numerical simulations (DNS) resolving all turbulence scales. The benchmark is performed for a confined backward-facing step flow at low Reynolds number. Hybrid models considered in the study are the scale-adaptive simulation model (SAS) and variants of the detached-eddy simulation model (DES).

2. CASE DESCRIPTION

We investigate an incompressible backward-facing step (BFS) flow, characterized by an inlet channel with a sudden step expansion. This expan-

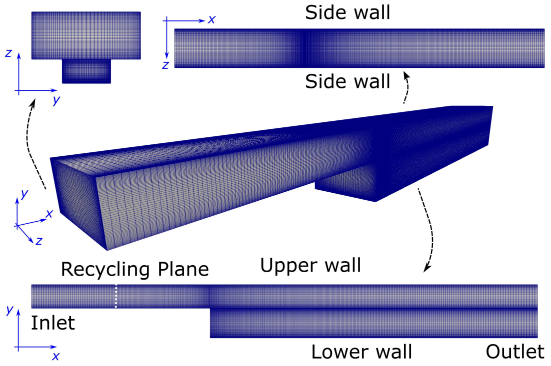

Figure 2. Overview of the baseline simulation grid.

sion results in adverse pressure gradients and a large-scale separated shear layer (SSL) downstream of the step, which in turn causes anisotropy and recirculation. Although the geometry is simple, these flow phenomena justify the BFS as a standard test case for turbulence models. We specifically focus on the reference BFS presented by Oder et al. [5]), for which a DNS database is available. A sketch of the considered BFS geometry is presented in Figure 1. Except for in- and outlet, all boundaries are solid walls, hence the BFS is confined. Upstream of the step, a recycling condition produces a fully developed channel flow with an inlet velocity $\langle u_{in} \rangle$. The flow is characterized by a relatively low Reynolds number $\mathrm{Re} = 6400$, based on $\langle u_{in} \rangle$ and step height h.

3. SIMULATION METHODOLOGY

3.1. Numerical setup

Incompressible simulations are compared for different turbulence models readily available in OpenFOAM v2012 [10, 11]. To this end, simulations are performed on an identical baseline simulation grid suitable for all turbulence modeling strategies considered, as illustrated in Figure 2. The wall resolution is chosen to resolve the viscous sublayers such that $y^+ = u_\tau y/\nu \approx 1$ averaged over solid surfaces, with u_τ the local friction velocity, y the first cell-center height off the wall, and ν the viscosity. The overall grid is further built with uniform stretching using the `simpleGrading` tool, such that resolution of large eddies remains supported throughout the domain, resulting in a grid of about 3.7 million cells. Initial tests showed that this grid supports LES in which about 94% of the turbulence in the domain is resolved, whereas the remaining 6% is accounted for by the subgrid-scale model. Matching the DNS reference setup, the inlet applies a 'mapped condition' which introduces the solution at the recycling plane back at the inlet, resulting in a periodic channel flow between inlet and recycling plane. Walls are treated with no-slip conditions (no wall functions are used), zero-gradient pressure, and appropriate fixed-value conditions for turbulence model quantities. At the outlet, a reference pressure value is fixed, whereas other flow quantities are subject to zero-gradient and zero-backflow conditions. Steady cases are solved using the simpleFoam solver, whereas the pisoFoam solver is used for transient simulations. Unsteady simulations are initialized using a steady RANS solution. Subsequently, simulations are advanced in time until a statistically stationary state is observed, after which statistical sampling is performed over a time horizon of about 50 domain flow-throughs.

3.2. Turbulence modeling

Baseline RANS and LES are performed as lower and upper limits of expected attainable performance by the hybrid models. The RANS uses the $k-\omega$ SST turbulence model [6], whereas the LES uses a high-fidelity dynamic k sub-grid scale model [7]. Both models rely on a prognostic equation for the modeled turbulent kinetic energy k. This prognostic equation contains a destruction term which is inversely proportional to a modeled turbulence length scale d. In this way, smaller values for d result in a reduction of modeled k, in turn yielding lower eddy viscosity ν_t. The main difference in governing equations of unsteady RANS and LES lies in the how d is defined. In RANS it depends solely on the solution as, e.g.,

$$d_{\mathrm{SST}} = k^{0.5}/(0.09\omega) \tag{1}$$

for the $k-\omega$ SST model. For LES on the other hand it is directly sensitized to the local grid resolution Δ as $d_{\mathrm{LES}} = C_{\mathrm{LES}}\Delta$ instead, with C_{LES} a constant in the order of 1 (dependent on local flow variables in dynamic formulations). In this way, on finer LES grids the foregoing ν_t reduction destabilizes the numerical solution to facilitate resolution of large eddies.

A first hybrid setup consists of the $k-\omega$ SST SAS turbulence model [8]. The SAS methodology can be viewed as an extension to unsteady RANS for which, in addition to the standard $k-\omega$ SST length scale d_{SST}, the underlying turbulence model is provided with a second independent von-Kármán length scale $d_{\nu K}$ based on the ratio of first and second-order velocity gradients. This allows to automatically reduce ν_t in regions of strong shear and inherent instability, thus promoting eddy resolution based solely on the properties of the numerical solution.

In contrast, the other three hybrid setups considered in this work lean more towards an LES approach, in which the grid resolution Δ plays a direct role in the turbulence model. More specifically, three variants of DES methods are considered. Firstly, we consider the $k-\omega$ SST DES developed by Strelets [2], which defines a length scale

$$d_{\mathrm{DES}} = \min\left(d_{\mathrm{SST}}, C_{\mathrm{DES}}\Delta\right). \tag{2}$$

Note that this results in DES adhering to the smallest of either the RANS or the LES length scale formulation[1], thus promoting LES behavior on sufficiently

[1] In practice, C_{DES} slightly differs from C_{LES} to accommodate different zones in the $k-\omega$ SST model.

Table 1. Overview of simulation cases.

Case	Resolution of large eddies	Turbulence model	Modeled turbulence length scale
RANS	None	$k-\omega$ SST [6]	$d_{\mathrm{SST}} = k^{0.5}/(0.09\omega)$
LES	Everywhere (down to grid scale Δ)	k (dynamic) [7]	$d_{\mathrm{LES}} = C_{\mathrm{LES}}\Delta$
SAS	Hybrid: based on solution	$k-\omega$ SST SAS [8]	$d_{\mathrm{SAS}} = d_{\mathrm{SST}}/d_{vK}$
DES	Hybrid: based on solution + grid	$k-\omega$ SST DES [2]	$d_{\mathrm{DES}} = \min(d_{\mathrm{SST}}, d_{\mathrm{LES}})$
DDES	Hybrid: DES + boundary-layer shielding	$k-\omega$ SST DDES [9]	$d_{\mathrm{DDES}} \approx d_{\mathrm{SST}}$ (close to walls) $\approx d_{\mathrm{DES}}$ (away from walls)
IDDES	Hybrid: DDES + WMLES features	$k-\omega$ SST IDDES [9]	$d_{\mathrm{IDDES}} \approx d_{\mathrm{SST}}$ (close to walls) $\approx d_{\mathrm{DES}}$ (away from walls) (+ log-layer modifications)

fine grids. Secondly, the $k-\omega$ SST Delayed DES formulation proposed by Gritskevitch *et al.* [9] is used. DDES defines a shielding function f_d, which is used to avoid spurious grid-induced transition to scale-resolving regimes in attached boundary layers, a problem which is known to severely impact accuracy in standard DES. The length scale is further defined as

$$d_{\mathrm{DDES}} = d_{\mathrm{SST}} - f_d \max\left(d_{\mathrm{SST}} - C_{\mathrm{DES}}\Delta\right), \tag{3}$$

with $f_d \approx 0$ close to walls, hence $d_{\mathrm{DDES}} \approx d_{\mathrm{SST}}$ and $f_d \approx 1$ away from them, resulting in $d_{\mathrm{DDES}} \approx d_{\mathrm{DES}}$. Third, the $k-\omega$ SST Improved DDES model is employed [9], which features slight modifications of DDES in the log layer close to solid boundaries to make it more amenable wall-modeled LES (WMLES) operation. Note that all turbulence models mentioned above are readily available in OpenFOAM v2012 and are used in their default configuration. Simulation cases for all 6 turbulence models considered here are summarized in Table 1.

4. RESULTS ON BASELINE GRID

In this section, we show the performance of the different turbulence models and compare them to each other and to the reference DNS data, with specific focus on the hybrid models. Firstly, we set the baseline performance by comparing the full RANS and LES approaches in Sect. 4.1. Next, we discuss the behavior of the different hybrid setups in Sect. 4.2. Finally, we discuss the overall performance of all methods in Sect. 4.3

4.1. Setting the bar: RANS and LES

A qualitative view of the flow fields in LES and RANS is shown in Figure 3. It can be seen that, while the RANS streamwise velocity is smooth and time-averaged by construction (a), the LES counterpart (b) features turbulent structures throughout the domain. Looking at the time-averaged vertical velocities in (c) and (d), the 3D structure of the fields is very different, especially in the downstream vicinity of the step.

Profiles of flow quantities along the domain mid-plane are compared to DNS data in Figure 4. For the horizontal velocity $\bar{u}$ (a), it can be seen that the turbulent channel profiles from DNS are matched well by both RANS and LES. However, downstream of

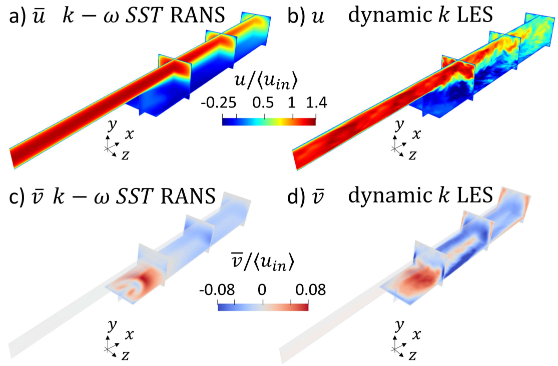

Figure 3. Flow field visualization for RANS (left, a, c) and LES (right, b, d) of streamwise velocity u (top, a, b) and vertical velocity v (bottom, c, d). All except (b) illustrate time-averaged quantities.

the step, RANS shows significant deviations from the DNS whereas LES retains a good match throughout the domain. More specifically, the backflow velocity in the separation bubble close to the step ($1 \le x/h \le 3$) is significantly underpredicted by RANS, whereas the flow velocity in the top right part of the domain is overpredicted ($3 \le x/h \le 11, 0 \le y/h \le 0.8$). Turning to the vertical velocity $\bar{v}$ in panel (b), it is seen that the LES achieves an acceptable match with the DNS data. Even though the velocity is lower than the DNS data for $4 \le x/h \le 10, -1 \le y/h \le 0$, the overall shape of the profile is retained. In contrast, RANS only matches the DNS profile at $x/h = 2$, while the S-shaped profiles observed in DNS and LES are not found at all in the RANS solution.

In addition to the mean-flow quantities discussed above, Figure 4c) contains profiles of the resolved and modeled time-averaged turbulent kinetic energy $\bar{k}$. LES achieves a good match with DNS, although slight overpredictions are observed for $2 \le x/h \le 4, -1 \le y \le 0$. Furthermore, the LES seems highly resolved, i.e., sub-grid modeled components are much smaller than the resolved components. Regarding the modeled turbulence in RANS, we see the largest discrepancies with DNS are observed in the SSL close to the step, where turbulence is generally underpredicted. Downstream, the match with DNS is improved, although it remains worse than the LES.

In summary, we conclude here that LES is able to match the DNS data throughout the entire domain, whereas RANS exhibits significant discrepancies downstream of the step. This observation is in line with the motivation for using hybrid RANS/LES turbulence models, as large-eddy scale resolution in the downstream zone could hence be capable of increasing overall accuracy.

4.2. Behavior of hybrid methods

4.2.1. SAS

Figure 5 shows a snapshot of streamwise velocity u (a) as well as the time-averaged vertical velocity (b). A first observation is that the streamwise velocity snapshot is free of any resolved turbulence fluctuations. Next, the vertical velocity in the case of SAS exhibits a similar structure as that in RANS shown in Figure 3c), which was discussed to match poorly with the DNS reference. Also upon investigation of the midplane profiles, which are not further shown here, the SAS was found to be nearly identical to RANS. Summarizing, in the current setup, SAS fails to resolve any turbulence and does not improve model fidelity over a standard RANS.

4.2.2. DES

As shown in Figure 6, the DES qualitatively behaves much like the LES from Figure 3(b,d), including a domain filled with turbulent fluctuations for the snapshot and a similar structure in vertical velocity as observed in the LES. Figure 7 illustrates the time-averaged RANS / LES indicator function, which is defined based on the modeled turbulence lengthscale (see Table 1) with the `DESModelRegions` function in OpenFOAM. It can be seen that the majority of the midplane is consistently treated as LES, while regions very close to the wall turn to a RANS approach. Only the region closely downstream of the step exhibits some switching between RANS and LES. Apart from the latter, the DES thus behaves very similar to a WMLES. This further explains the observations in midplane profiles in Figure 8, showing strong similarity between LES and DES, except very close to the step, where DES underpredicts both the vertical velocity $\overline{v}$ and the turbulence kinetic energy $\overline{k}$.

4.2.3. DDES

DDES has been originally designed to avoid the transition to LES mode in wall-attached boundary layers. Figure 9a) indicates that the channel region does not contain any fluctuations, and that the onset of scale resolution is delayed to the far downstream region of the SSL. The RANS / LES indicator function shown in Figure 10 indeed reveals a hybrid domain division into a RANS zone in the upstream channel and top-wall attached boundary layer, whereas the SSL is treated with LES. This domain partitioning is highly desirable, since RANS was shown to work well in such regions and expected to allow significant grid coarsening, whereas LES should enhance fidelity in the SSL. However, when comparing the vertical velocity structure in Figure 9b), we see that neither of the expected structures observed before in RANS or LES is attained.

Further looking at midplane profiles in Figure 8, DDES produces a poor match with DNS / LES. The expected recirculation zone ($0 \leq x/h \leq 6, -1 \leq y/h \leq 0$) appears to be almost stagnant with no recirculation predicted by DDES. Furthermore, the vertical velocity is very much underpredicted in this zone, which seems to be compensated by far too large negative vertical velocities in the outlet zone ($x/h \geq 8$). Focusing on turbulence profiles in Figure 8c), it becomes clear that DDES is suffering from severe MSD in the expected recirculation zone. Even though the model has turned to an LES formulation here (thus without support of a RANS turbulence model), this zone is turbulence-deficient without any resolved scales to take up the turbulent mixing effects. Possibly the relatively low Reynolds number is delaying transition at the separation point.

4.2.4. IDDES

IDDES was developed as a DDES formulation that would be more amenable to WMLES. Figure 11 shows the flow field to be very similar to fields from LES and DES (which was shown to behave as WMLES). Interestingly, the shielding functions do not prohibit LES zones in the upstream channel flow, but do created a RANS zone immediately adjacent to the step separation point as shown in Figure 12. Midplane profiles shown in Figure 11 further confirm the affinity to LES results.

4.3. Discussion

In the previous sections, a qualitative discussion and comparison of the flow fields of the considered models was performed. A comparison between steady RANS and LES showed that large-eddy resolution in the SSL allows to significantly improve the overall match with DNS data, justifying that the current BFS setup is suitable for testing the performance of locally scale-resolving hybrid methods.

Results obtained from the hybrid simulation indicated that for the current case their behavior can be classified in three groups. Firstly, SAS resembles a steady RANS field, with virtually no scale resolution and similar flow field characteristics. Secondly, DES and IDDES behave like WMLES, where the entire domain is simulated as an LES zone, except for regions in the direct wall vicinity. Thirdly, DDES exhibits a more classical hybrid domain subdivision, in which only the SSL is an LES zone, whereas the inlet channel and top wall are predominantly RANS. This latter configuration is promising, as it turns to scale resolution only in the region where RANS clearly struggles to match the DNS data. The different behavior between DDES and IDDES (which are formulated in a relatively similar manner) is an interesting

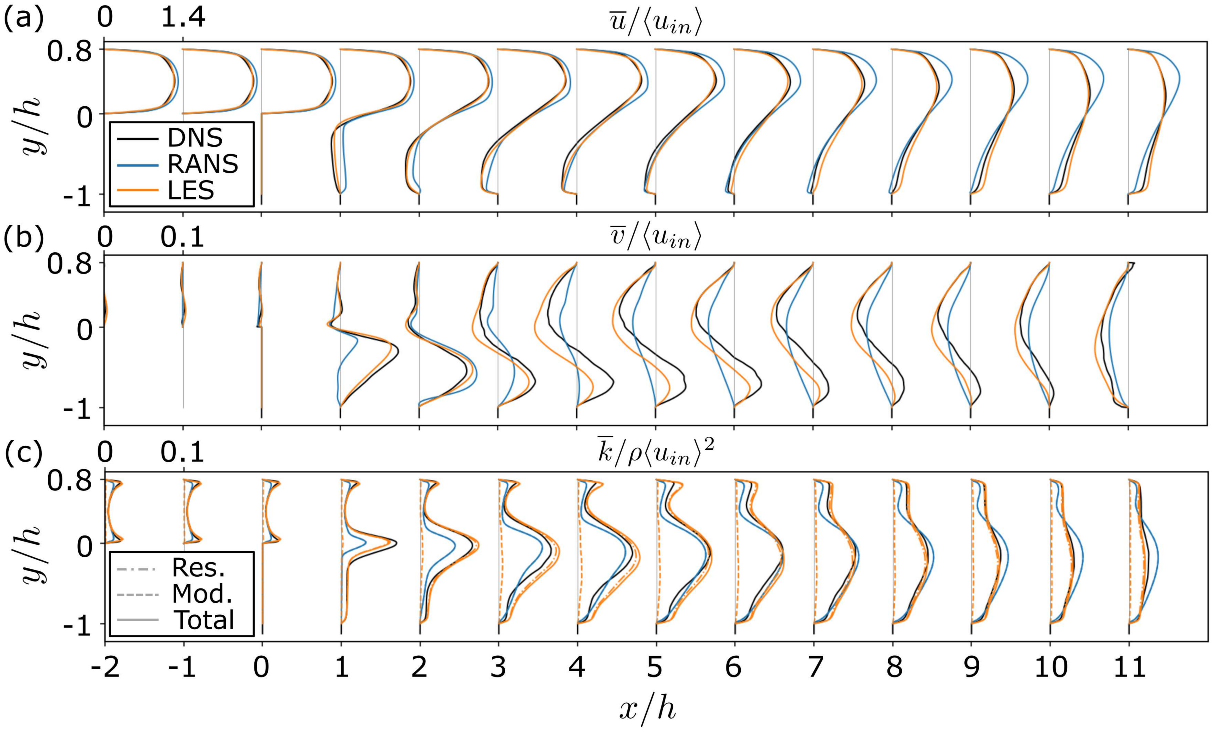

Figure 4. Profiles along midplane for DNS, RANS, and LES. (a) Streamwise velocity component $\overline{u}$. (b) Vertical velocity component $\overline{v}$. Turbulent kinetic energy $\overline{k}$. Dashed, dot-dashed, and full lines indicated modeled, resolved and total (modeled + resolved) components. (Modeled and resolved components in DNS and RANS respectively are zero by definition and not further shown).

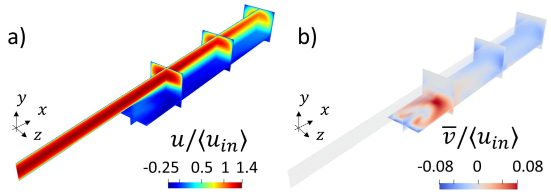

Figure 5. Flow field visualization for SAS. a) Streamwise velocity snapshot u. b) Time-averaged vertical velocity $\overline{v}$.

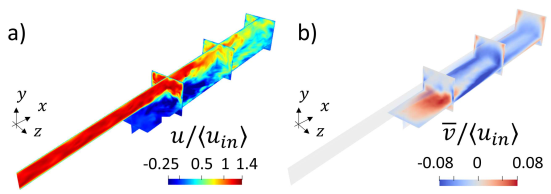

Figure 6. Flow field visualization for DES. a) Streamwise velocity snapshot u. b) Time-averaged vertical velocity $\overline{v}$.

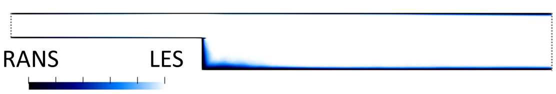

Figure 7. RANS/LES indicator function along the midplane for the DES setup.

observation, possibly indicating a sensitive bifurcation in the behavior of these methods for this setup.

Table 2 provides a quantitative comparison of all considered turbulence models based on the relative mean absolute error (MAE) of profiles with respect to DNS shown in the discussions above. A first observation is that the vertical velocity $\overline{v}$ generally exhibits the largest error. Next, we see that general qualitative observations from previous sections are reaffirmed here, i.e. LES has the lowest MAE overall for every variable, whereas RANS shows significantly larger MAE than LES. SAS does not significantly improve the accuracy in comparison to RANS, while the WMLES-like behavior of DDES and IDDES result in important error reduction, more specifically for $\overline{u}$ and $\overline{v}$ Finally, DDES, even though it shows a promising RANS / LES domain partition, has the poorest accuracy of all simulations, caused by the MSD resulting from a delayed transition of the separated shear layer downstream of the step.

A recurring observation throughout Sect. 4 has been the different structure of both vertical and backflow velocity close to the step, which suggests a different organization of the recirculation and reattachment in the different simulations. To quantify this, we compute the time- and spanwise-averaged wall shear stress $\overline{\tau}$ at the bottom surface downstream of the step as

$$\overline{\tau}/\rho = \frac{1}{TL_z} \int_0^{L_z} \int_0^T \tau_{\mathrm{wall}}(x,z,t)/\rho \, \mathrm{d}t \, \mathrm{d}z, \tag{4}$$

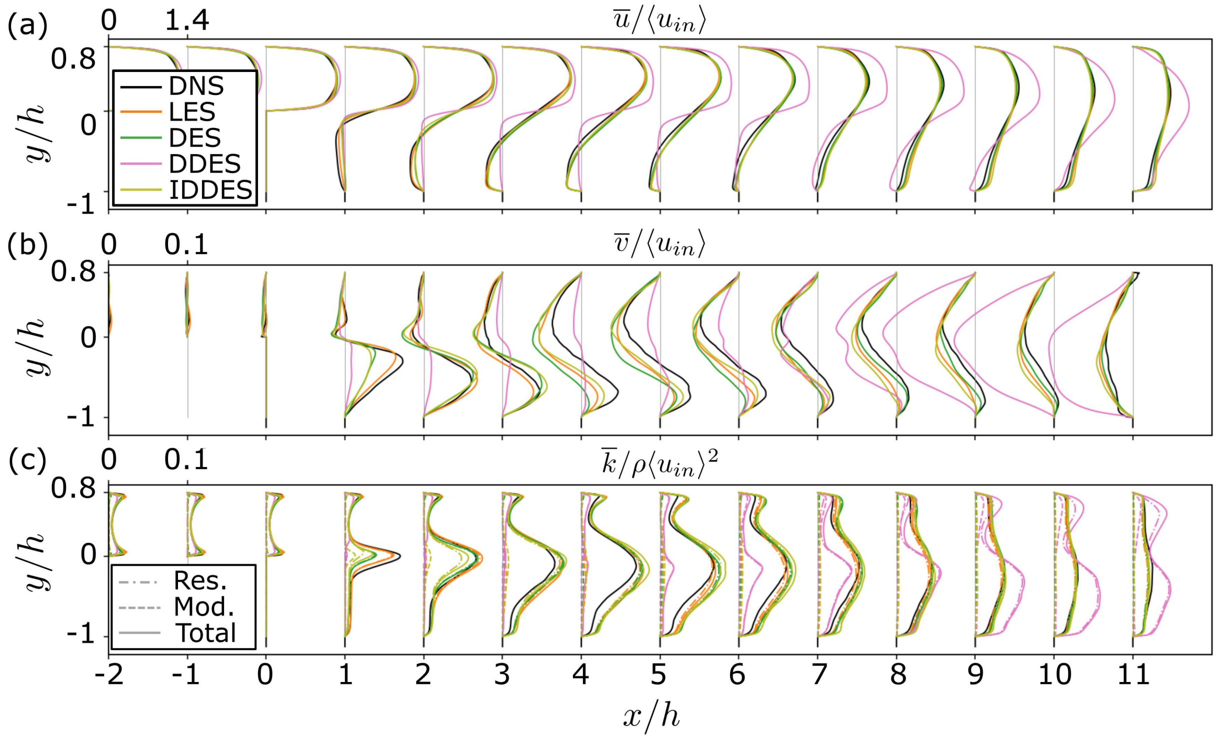

Figure 8. Profiles along midplane for DNS, LES, and DES variants. (a) Streamwise velocity component $\overline{u}$. (b) Vertical velocity component $\overline{v}$. Turbulent kinetic energy $\overline{k}$. Dashed, dot-dashed, and full lines indicated modeled, resolved and total (modeled + resolved) components.

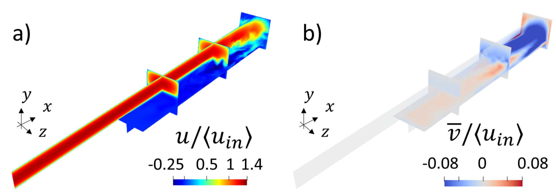

Figure 9. Flow field visualization for DDES. a) Streamwise velocity snapshot u. b) Time-averaged vertical velocity $\overline{v}$.

Figure 10. RANS/LES indicator function along the midplane for the DDES setup.

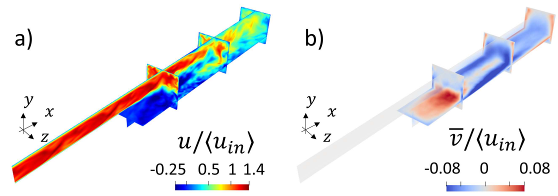

Figure 11. Flow field visualization for IDDES. a) Streamwise velocity snapshot u. b) Time-averaged vertical velocity $\overline{v}$.

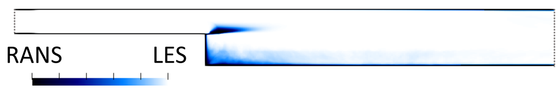

Figure 12. RANS/LES indicator function along the midplane for the IDDES setup.

which is plotted as a function of streamwise location in Figure 13. The zero-crossing of $\overline{\tau}$ represents a spanwise-averaged reattachment point. LES, DES, and IDDES, reaffirm their resemblence and fidelity by closely matching the reattachment point observed in the reference DNS. Also, RANS and SAS are both shown to severely overpredict the size of the recirculation bubble, with RANS reattaching at $x/h \approx 11$, and SAS not reattaching at all. DDES finally shows a different recirculation structure from any of the other models, caused by the MSD mentioned above.

5. GRID RESOLUTION SENSITIVITY

An important note to make on the results presented in the previous section is they are all performed on a fine mesh suitable for highly-resolved LES, as shown by the minor contribution of sub-grid LES terms e.g. in Figure 4. Therefore, the computational cost of all simulations (except for the steady RANS) is roughly equal. However, an appeal of hybrid and RANS methods is that they potentially retain their accuracy on more affordable meshes, since RANS zones are more robust to coarse resolutions than LES.

For this reason, we present a grid study here, and

Table 2. Relative mean absolute error of mid-plane profiles compared to DNS reference [5]. Best and worst values for every variable are indicated in boldfaced and underlined text respectively.

Model	$\overline{u}$	$\overline{v}$	$\overline{k}$
RANS	7.3%	16.0%	9.0%
SAS	9.7%	15.5%	8.9%
DES	3.9%	12.9%	7.2%
DDES	12%	32.0%	22.7%
IDDES	4.1%	12.2%	8.7%
LES	**2.8%**	**8.8%**	**5.5%**

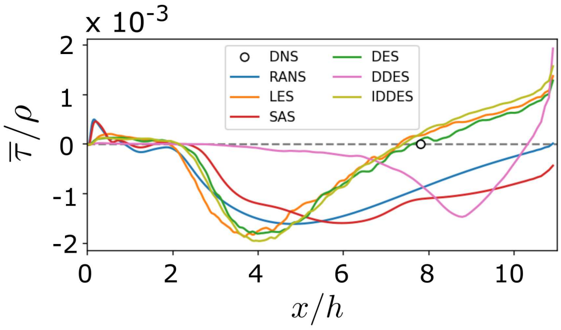

Figure 13. Time- and spanwise-averaged wall shear stress for RANS, LES, SAS, DES, DDES, and IDDES. DNS reattachment shown with circle.

quantify error sensitivity of different turbulence models to grid coarsening. The study is performed with 6 coarsened grids (C1 – C6), where the baseline grid resolution is reduced by 20% in all spatial directions, resulting in an overall reduction of degrees of freedom by a factor about 2 per coarsening step, or a total reduction of about 160 over the entire range.

A first observation from Table 3 (top) is the insensitivity of RANS error of about 9.6% to the grid resolution over the large range of coarsening. On the other side of the spectrum, we see that LES shows an expected decrease in accuracy with grid coarsening, as fewer turbulent scales can be resolved by the grid and have to be accounted for by the subgrid-scale model. Based on the current error metric, the crossover point, where RANS attains similar or superior accuracy over LES, lies around a resolution between the C3 grid and C4 grid. It was found that, around this point, the domain-integrated fraction of resolved to total turbulent kinetic energy in LES is about 80% for these grids, corresponding with the general 80% rule-of-thumb for a proper LES. These are promising observations especially for the LES-like hybrid methods DES, DDES and IDDES, as grid coarsening could convert LES zones to RANS zones, and it is observed that in RANS zones the grid resolution, and hence the computational cost, can significantly reduced without sacrificing accuracy.

However, investigation of the hybrid performance shows that this promise remains unfulfilled, as none of the hybrid methods can retain accuracy higher than the RANS baseline error of 9.6% upon grid coarsening. DDES remains very poor for all grids considered. DES exhibits a sharp error increase for grid C2. Further investigation showed this was caused by a laminarization of the inlet channel in LES mode. Indeed, Table 3 (bottom) shows that DES retains its WMLES character and does not switch to RANS zones, even at the coarsest grids. IDDES shows a gradual increase in errors due to a switch towards the configuration with RANS at inlet and walls, and LES in the SSL. However, in this mode IDDES suffers from MSD, resulting in large errors.

The observations in the current section allow to draw important conclusions regarding the hybrid methods considered in this report for the current low-Reynolds number BFS flow. Although for LES-suited grids DES and IDDES improve the match with DNS data compared to the baseline RANS by running in WMLES mode, these improvements are not retained upon grid coarsening. SAS and DDES never succeed to surpass RANS accuracy. Note that some of these observations can be linked to the relatively low Reynolds number of the current setup. We verified that, at higher Reynolds numbers the foregoing problems are somewhat mitigated, yet not fully resolved. This is omitted here due to space limitations.

6. SUMMARY

We have investigated hybrid turbulence models for a confined BFS flow at low Reynolds number. Simulations were performed using RANS, LES, and hybrid SAS and DES variants. Results were compared to existing high-fidelity DNS data. A first set of simulations was performed on a fine simulation grid. A comparison between RANS and LES showed that partial scale resolution allows to significantly improve the overall match with DNS, justifying the current BFS setup is suitable for testing the performance of locally scale-resolving hybrid methods. Results obtained from the hybrid simulations indicate that, for the current case, their behavior can be classified in three groups, with SAS resembling RANS, DES and IDDES behaving like WMLES, and DDES showing a more promising hybrid domain partition.

A quantitative comparison revealed that the (WM)LES type models DES and IDDES emerge as the higher-fidelity hybrid turbulence models. In contrast, SAS and DDES fail to consistently improve over RANS. Especially the recirculation structure and associated reattachment point are very ill-predicted by the SAS and DDES, whereas DES and IDDES closely adhere to the LES and DNS. While SAS does not qualitatively distinguish itself from RANS, the DDES suffers from MSD caused by a lack of both resolved and modeled turbulence in the zone close to the step.

A grid coarsening study was performed to quantify the error degradation of all models, as well as the switching behavior between RANS and LES

Table 3. Top: *Averaged error metric* for sensitivity study including baseline (B) and coarsened grids (C1 – C6). Degrees of freedom per grid are shown in parenthesis. Best and worst errors for every grid indicated in boldfaced and underlined text respectively. Bottom: *Domain LES fraction* for DES, DDES, and IDDES. Boldfaced text indicates configuration with RANS at inlet and walls combined with LES in SSL

	B	C1	C2	C3	C4	C5	C6
Averaged error metric	(3.7M)	(1.9M)	(942k)	(465k)	(230k)	(106k)	(52k)
RANS	9.6%	9.8%	9.9%	9.8%	**9.9%**	**9.5%**	**9.5%**
SAS	10.4%	10.8%	11.2%	11.3%	10.3%	9.9 %	9.9%
DES	7.3%	10.8%	23.0%	21.9%	21.3%	20.9%	19.1%
DDES	20.1%	18.3%	21.9%	17.4%	18.0%	18.0%	17.6%
IDDES	8.0%	10.4%	12.0%	11.7%	15.9%	16.6%	14.6%
LES	**6.2%**	**8.2%**	**8.7%**	**9.5 %**	11.5%	12.4%	13.3%
Domain LES fraction	B	C1	C2	C3	C4	C5	C6
DES	87%	86%	56%	57%	57%	61%	67%
DDES	**41%**	**38%**	56%	**31%**	**30%**	**31%**	**27%**
IDDES	88%	87%	85%	**33%**	**36%**	**34%**	**26%**

zones for DES and its variants. The grid study showed that, although its error metrics continuously worsen with coarsening, LES retains superior accuracy over RANS except for very coarse grids. However, none of the hybrid methods retained their improvements over RANS for coarsened grids.

In conclusion, it was shown that, for the current setup, the considered hybrid methods only perform adequately if the grid allows them to run in WMLES mode throughout the entire domain, and that attempts to reduce computational cost with regard to a full LES invariably lead to a strong increase in error for the hybrid models. However, also more promising observations were made, mainly that DDES and IDDES are capable of automatically dividing the domain into desirable RANS and LES zones, and that higher Reynolds numbers appear to promote scale development closer to the step.

We close with suggestions for future research. A similar investigation for significantly higher Reynolds numbers will clarify whether current models automatically improve by earlier natural scale development. Also, it would be interesting to see whether scale development is promoted by perturbations close to the separation point, or whether such immediate development can only be attained by resolved turbulence in the channel, which triggers a bypass-type transition in the SSL. Finally, it is important to note that we only considered ready-to-use standard hybrid techniques available in OpenFOAM v2012. It would be interesting to further assess the behavior of more advanced hybrid models that promise rapid transition in separated flows for the current BFS setup [12].

ACKNOWLEDGEMENTS

The authors thank Jure Oder and Matilde Fiore for discussions and help with the DNS data. This work has been performed in context of the PATRICIA project, which has received funding from European Union's Horizon 2020 Research and Innovation programme under grant agreement No. 945077.

REFERENCES

[1] Spalart, P. R., 2009, "Detached-eddy simulation", *Annual review of fluid mechanics*, Vol. 41, pp. 181–202.

[2] Strelets, M., 2001, "Detached eddy simulation of massively separated flows", *39th Aerospace sciences meeting and exhibit*, p. 879.

[3] Chaouat, B., 2017, "The state of the art of hybrid RANS/LES modeling for the simulation of turbulent flows", *Flow, turbulence and combustion*, Vol. 99 (2), pp. 279–327.

[4] Tiselj, I., and Oder, J., 2019, "Direct Numerical Simulation of a Backward-Facing Step.", *Technical Deliverable of Euratom RIA SESAME project*.

[5] Oder, J., Shams, A., Cizelj, L., and Tiselj, I., 2019, "Direct numerical simulation of low-Prandtl fluid flow over a confined backward facing step", *International Journal of Heat and Mass Transfer*, Vol. 142, p. 118436.

[6] Menter, F. R., Kuntz, M., and Langtry, R., 2003, "Ten years of industrial experience with the SST turbulence model", *Turbulence, heat and mass transfer*, Vol. 4 (1), pp. 625–632.

[7] Kim, W.-W., and Menon, S., 1995, "A new dynamic one-equation subgrid-scale model for large eddy simulations", *33rd Aerospace Sciences Meeting and Exhibit*, p. 356.

[8] Egorov, Y., and Menter, F., 2008, "Development and application of SST-SAS turbulence model in the DESIDER project", *Advances in Hybrid RANS-LES Modelling*, Springer, pp. 261–270.

[9] Gritskevich, M. S., Garbaruk, A. V., Schütze, J., and Menter, F. R., 2012, “Development of DDES and IDDES formulations for the k-ω shear stress transport model”, *Flow, turbulence and combustion*, Vol. 88 (3), pp. 431–449.

[10] OpenCFD OpenFOAM v2012, available at `https://develop.openfoam.com/Development/openfoam/-/releases/OpenFOAM-v2012`, accessed: 24 May 2022.

[11] Weller, H. G., Tabor, G., Jasak, H., and Fureby, C., 1998, “A tensorial approach to computational continuum mechanics using object-oriented techniques”, *Computers in Physics*, Vol. 12 (6), pp. 620–631.

[12] Shur, M. L., Spalart, P. R., Strelets, M. K., and Travin, A. K., 2015, “An enhanced version of DES with rapid transition from RANS to LES in separated flows”, *Flow, turbulence and combustion*, Vol. 95 (4), pp. 709–737.